Rapid and Efficient Generation of Functional Motor Neurons From Human Pluripotent Stem Cells Using Gene Delivered Transcription Factor Codes

Mark E Hester[1], Matthew J Murtha[1,2], SungWon Song[1], Meghan Rao[1], Carlos J Miranda[1], Kathrin Meyer[1], Jinbin Tian[3], Gabriella Boulting[4–6], David V Schaffer[7], Michael X Zhu[3], Samuel L Pfaff[8], Fred H Gage[9] and Brian K Kaspar[1–3]

[1]Center for Gene Therapy, The Research Institute at Nationwide Children's Research Institute, Columbus, Ohio, USA; [2]Molecular, Cellular and Developmental Biology Program, The Ohio State University, Columbus, Ohio, USA; [3]Department of Neuroscience and the Center for Molecular Neurobiology, The Ohio State University, Columbus, Ohio, USA; [4]The Howard Hughes Medical Institute, Cambridge, Massachusetts, USA; [5]Harvard Stem Cell Institute, Department of Stem Cell and Regenerative Biology, Harvard University, Cambridge, Massachusetts, USA; [6]Department of Molecular and Cellular Biology, Harvard University, Cambridge, Massachusetts, USA; [7]Department of Chemical Engineering and the Helen Wills Neuroscience Institute, University of California, Berkeley, California, USA; [8]Howard Hughes Medical Institute and Gene Expression Laboratory, The Salk Institute for Biological Studies, La Jolla, California, USA; [9]Laboratory of Genetics, The Salk Institute for Biological Studies, La Jolla, California, USA

Stem cell-derived motor neurons (MNs) are increasingly utilized for modeling disease *in vitro* and for developing cellular replacement strategies for spinal cord injury and diseases such as spinal muscular atrophy (SMA) and amyotrophic lateral sclerosis (ALS). Human embryonic stem cell (hESC) differentiation into MNs, which involves retinoic acid (RA) and activation of the sonic hedgehog (SHH) pathway is inefficient and requires up to 60 days to develop MNs with electrophysiological properties. This prolonged differentiation process has hampered the use of hESCs, in particular for high-throughput screening. We evaluated the MN gene expression profile of RA/SHH-differentiated hESCs to identify rate-limiting factors involved in MN development. Based on this analysis, we developed an adenoviral gene delivery system encoding for MN inducing transcription factors: neurogenin 2 (Ngn2), islet-1 (Isl-1), and LIM/homeobox protein 3 (Lhx3). Strikingly, delivery of these factors induced functional MNs with mature electrophysiological properties, 11-days after gene delivery, with >60–70% efficiency from hESCs and human induced pluripotent stem cells (hiPSCs). This directed programming approach significantly reduces the time required to generate electrophysiologically-active MNs by approximately 30 days in comparison to conventional differentiation techniques. Our results further exemplify the potential to use transcriptional coding for rapid and efficient production of defined cell types from hESCs and hiPSCs.

Received 19 March 2011; accepted 8 June 2011; published online 19 July 2011. doi:10.1038/mt.2011.135

INTRODUCTION

Recent progress in cell-based modeling using human embryonic stem cell (hESC) and induced pluripotent stem cell-(iPSC)-derived motor neurons (MNs) has opened new opportunities to understand the development of the motor system as well as MN disease. MNs are a highly specialized class of neurons that reside in the spinal cord and project axons in organized and discrete patterns to muscles to control their activity. The most prominent MN diseases are spinal muscular atrophy (SMA) and amyotrophic lateral sclerosis (ALS), in which MNs perish in the disease. In the case of SMA, the genetic deficit of reduced SMN levels is known. Indeed gene delivery of *SMN* in a transgenic model of SMA results in prolonged survival and motor rescue, indicating that methods to increase SMN levels in MNs may be therapeutic.[1–4] Stem cell-derived MNs have been derived from iPSCs from a SMA patient, providing a new population of cells for drug and therapeutic screens.[5] In addition, stem cell-based therapies have also demonstrated therapeutic potential in SMA and spinal cord injury. For example, studies have reported that transplanting MN progenitor cells into the spinal cords of SMA mice or into a spinal cord injured rat model partially restores motor decline.[6,7] MNs have also been extensively utilized to study ALS and screen potential therapeutic compounds,[8–13] thereby demonstrating the requirements for generating large numbers of MNs.

To generate large numbers of spinal MNs for use in *in vitro*-based screens and transplantation studies, neuromuscular researchers have taken advantage of the propensity of mouse ESCs to efficiently differentiate into this cell type. However, progress repeating these studies with hESCs has been slow due to the low efficiency of MN production and tedious, time-consuming culture conditions. The current procedures for generating MNs involve embryoid body formation in serum-free media and subsequent neural rosette formation in the presence of retinoic acid (RA) and sonic hedgehog (SHH), which function to caudalize and ventralize MN progenitors,[14,15] respectively. Neurotrophic factors are then added to the medium for further maturation and to aid in cell survival. The entire differentiation process requires up to 2 months to generate MNs, which are electrophysiologically-active,

Correspondence: *Brian K Kaspar, 700 Children's Drive, WA3022, Columbus, Ohio 43205, USA. E-mail: Brian.Kaspar@NationwideChildrens.org*

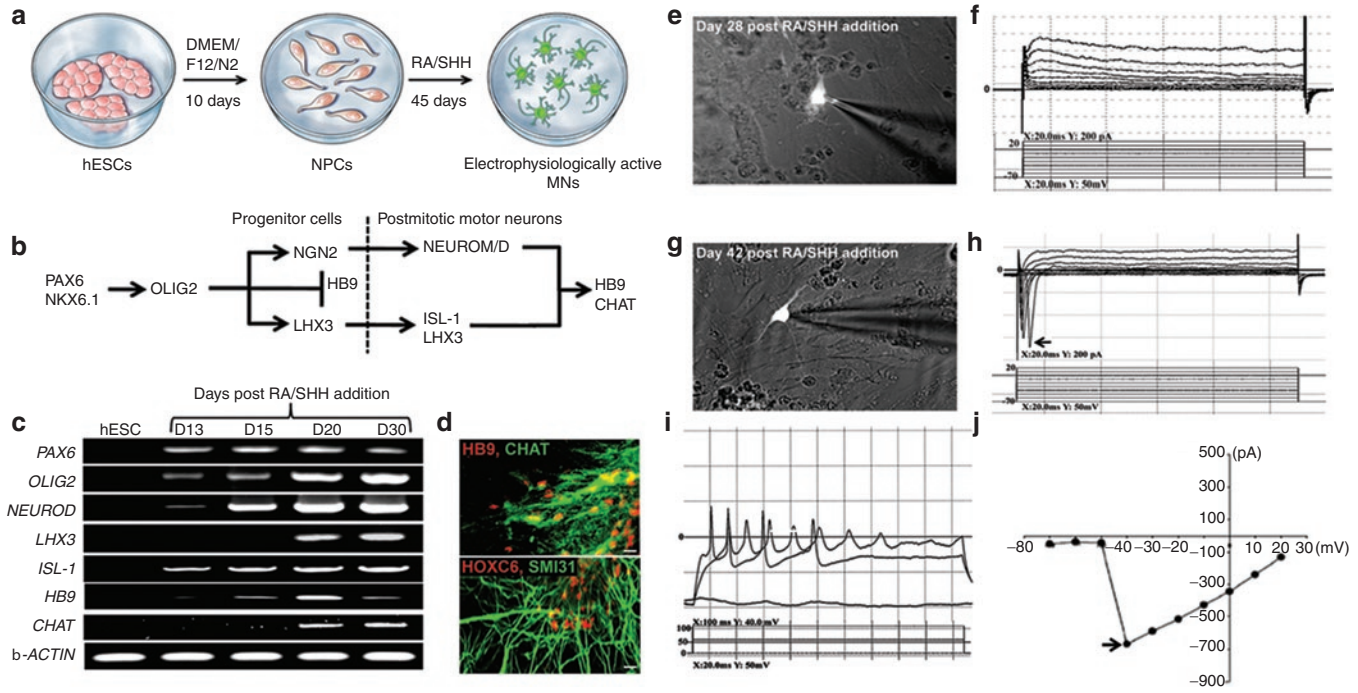

Figure 1 hESCs require a long differentiation and maturation period to differentiate into functional MNs *in vitro*. (**a**) Differentiation paradigm of hESCs into MNs. hESCs were differentiated into neural progenitor cells in DMEM/F12/N2 media followed by RA/SHH treatment to induce MN differentiation. (**b**) Schematic depicting critical signaling factors in MN development. (**c**) RT-PCR analysis of markers involved in early and late MN differentiation assayed at multiple time points post RA/SHH treatment. (**d**) Mature MNs coexpress HB9 (red) and CHAT (green), and also express SMI31 (green) and express a marker of cervical spinal cord identity, HOXC6 (red). (**e**) Patch-clamped *Hb9::RFP* MN at 28 days post RA/SHH addition showed no sodium current activity (**f**). (**g**) Patch-clamped *Hb9::RFP* MN 2 weeks later showed sodium current activity (**h**), action potentials (**i**), and peak sodium current activity of approximately −700 pA (**j**). Arrow in panel "**h**" shows peaks representing sodium currents. Arrow in panel "**j**" shows the peak sodium current activity. In panel "**d**" bar = 50 µm. CHAT, choline acetyltransferase; DMEM, Dulbecco's modified Eagle's medium; hESCs, human embryonic stem cells; MN, motor neurons; RA, retinoic acid; RT-PCR, reverse transcriptase-PCR; SHH, sonic hedgehog.

with 10–40% efficiency.[16–21] To gain insight into the barriers to MN differentiation, we evaluated the gene expression profile of MN codes in RA/SHH-treated cells temporally to determine which factors were rate-limiting in the process. After identifying these rate-limiting factors, we utilized an adenoviral gene delivery strategy to rapidly induce expression of MN codes: neurogenin 2 (NGN2), islet-1 (ISL-1), and LIM/homeobox protein 3 (LHX3) in both hES and hiPS cells. Our differentiation strategy to generate induced MNs from human pluripotent stem cells could be utilized for *in vitro* MN disease modeling platforms or as a potential source for cell-based therapies.

RESULTS

RA/SHH induction of MNs from hESCs requires a long differentiation and maturation period

For our initial studies, we utilized the HSF-6 hESC cell line, which was confirmed to have a normal karyotype throughout the course of these studies (**Supplementary Figure S1**). In addition, these cells expressed high levels of alkaline phosphatase and transcription factors involved in pluripotency such as REX1, OCT3/4, NANOG, and SOX2, as assessed by immunohistochemistry and reverse transcriptase-PCR (RT-PCR) (**Supplementary Figure S2a–c**). This line also expressed a cell surface marker unique to hESCs, SSEA4, as shown by immunocytochemical analysis (**Supplementary Figure S2c**), demonstrating that our cells expressed markers for *bona fide* pluripotent stem cells. To confirm that the HSF-6 cell line could produce MNs, we utilized the prototypical methods of ectopically administering RA and SHH to signal MN development pathways,[16,18,22] (**Figure 1a–b**). The HSF6-hESCs could be induced into a neuroectodermal fate, as previously described,[22,23] with >70% of cells positive for neural progenitor cell (NPC) markers PSA-NCAM and OTX2 (**Supplementary Figure S3**). We then evaluated the MN gene expression profile by semi-quantitative RT-PCR to characterize the timing for MN activation (**Figure 1c**). Following addition of RA and SHH to embryoid body cultures, we analyzed the transcriptional program that induces MN formation (**Figure 1b**) temporally over 30 days by semi-quantitative RT-PCR (**Figure 1c**). In proliferating hESCs, no neuronal specifying factors were present in our cultures, suggesting a homogeneous population of undifferentiated cells. At day 13 of differentiation, we observed expression of early MN-specifying factors, PAX6 and OLIG2 as well as ISL-1 and NEUROD (**Figure 1c**). Immunocytochemical analysis also confirmed the expression of the former three markers (**Supplementary Figure S3**). Expression of all MN-specifying genes was evident at day 20 and day 30, including strong expression of LHX3, ISL-1, and HB9 (**Figure 1c**). Twenty days after RA/SHH, choline acetyltransferase (CHAT) expression appeared and increased at day 30. Immunohistochemistry confirmed the expression of endogenous HB9, LHX3, ISL-1, and CHAT, indicating that these cells were indeed expressing prototypical markers of MNs (**Figure 1d**, **Supplementary Figure S3**). Quantification of HB9^{+}

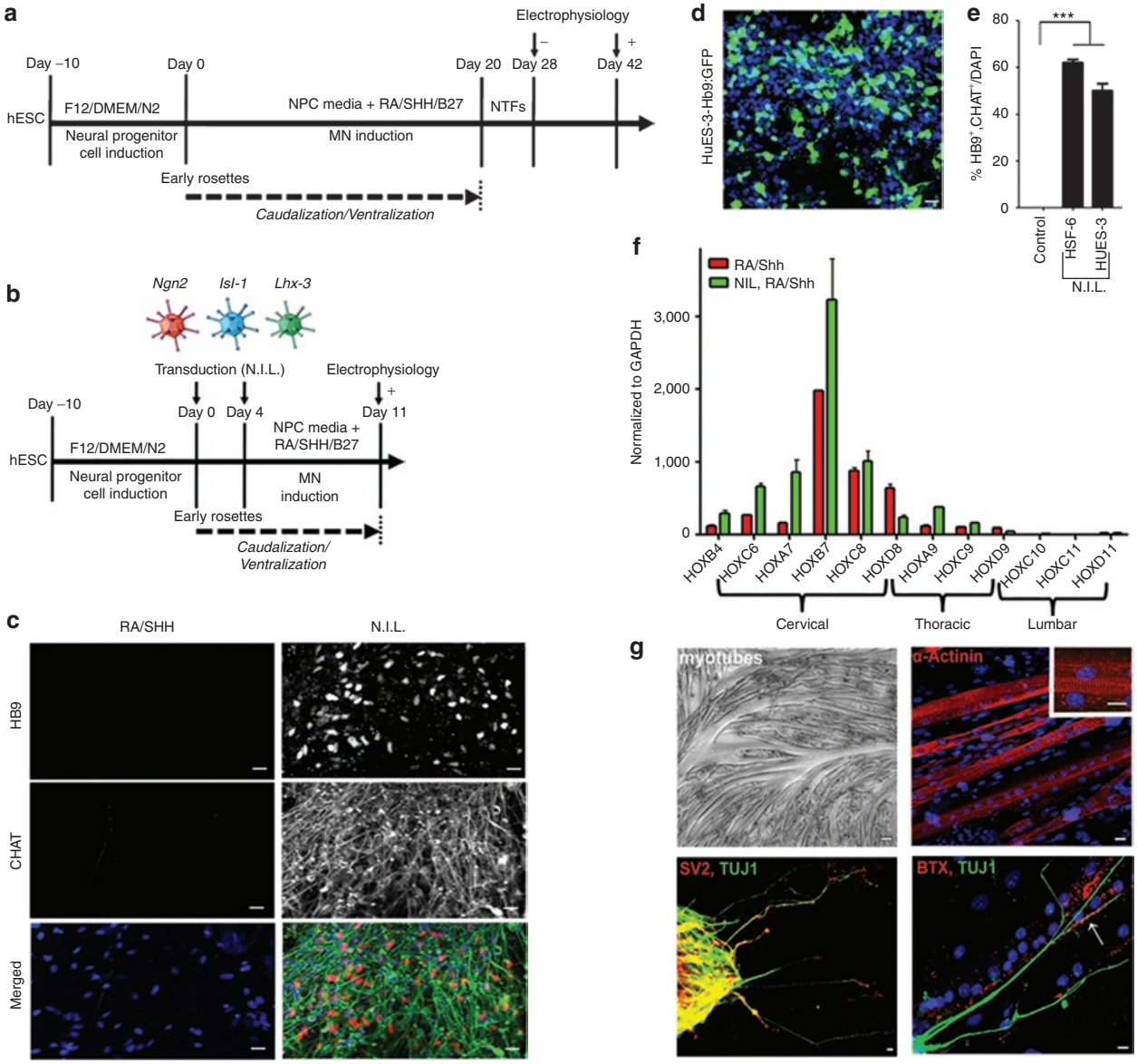

Figure 2 Rapid and efficient MN differentiation of hESCs by the N.I.L. transcription factors. (**a**) Time line of differentiating human ES or iPS cells towards electrophysiologically-competent MNs utilizing RA/SHH. (**b**) Time line of accelerating human ES or iPS cell differentiation towards electrophysiologically-competent MNs utilizing N.I.L. (**c**) N.I.L.-induced MN differentiation showed co-expression of mature MN markers HB9 and CHAT. (**d**) HuES-3 Hb9::GFP cells differentiated into MNs with the N.I.L. transcription factor code show GFP expression. (**e**) Quantification of colabeled HB9/CHAT induced MNs. (**f**) qRT-PCR analysis of *HOX* genes expressed in the cervical, thoracic, and lumbar regions of the spinal cord assayed from N.I.L.-induced MNs and RA/SHH-induced MNs. (**g**) Phase contrast picture of C2C12-derived myotubes, which express α-actinin, with a high-power insert showing characteristic striations. (**g**) N.I.L.-induced MNs express SV2 (red) and colocalize with axons labeled with TUJ1 (green). MN axon terminals form junctions with acetylcholine receptors labeled with bungarotoxin (Red) as shown by an arrow (bottom panel). Arrow in panel "**g**" shows the colocalization of a MN axon with acetylcholine receptors on a myotube. In panel "**c**" all bars = 50 µm. In panel "**g**" all bars = 20 µm. DMEM, Dulbecco's modified Eagle's medium; hESCs, human embryonic stem cells; MN, motor neurons; N.I.L., Ngn2, Isl-1, and Lhx3; RA, retinoic acid; qRT-PCR, quantitative reverse transcriptase-PCR; SHH, sonic hedgehog.

and CHAT$^+$ cells showed ~30% of total cells were indeed mature MNs, an efficiency similar to prior reports of hESC differentiation into MNs.[17–19] In addition, the hESC-derived MNs expressed SMI31, a nonphosphoryated neurofilament as well as HOXC6, demonstrating cervical MN identity, as expected (**Figure 1d**).[17] Collectively, these results exhibit a slow maturation process of RA/SHH-induced cells into a MN phenotype.

To determine whether the neurons in our cultures, which expressed mature MN markers, were indeed functionally mature, we analyzed their electrophysiological properties to test whether they could fire action potentials. Specifically, we utilized whole-cell perforated patch recording techniques to determine whether they developed the fast inactivating sodium currents and action potentials indicative of mature MNs.[24] To easily identify MNs in live cultures, a previously reported lentivirus reporter[13] encoding a red fluorescent protein (RFP) under the control of the MN-specific *Hb9* promoter was utilized. Transduced MNs were easily visualized by strong RFP expression throughout the whole-cell body and

neuritic extensions (**Figure 1e,g**). We first evaluated the electrophysiological properties of our differentiated MN cultures at day 28, an approximate time point in which we observed high expression levels of HB9 and CHAT. Interestingly, all six recorded MNs at this time point, which had been cultured on astrocytes for an additional 4 days in the presence of neurotrophic factors for further maturation[25] were not electrophysiologically mature, despite expressing all of the phenotypic markers for a MN, as no patch-clamped Hb9-RFP+ MN fired action potentials (**Figure 1e–f**, **Figure 2a**). This observation suggested additional maturation was required to induce the electrophysiological machinery proteins required for MNs to fire action potentials. Therefore, we cocultured these MNs for an additional 2 weeks on human astrocytes in the presence of RA/SHH and neurotrophic factors. At 42 days post RA/SHH treatment, a total of four *Hb9::RFP*-positive MNs were patch clamped in culture (**Figure 1g**) and a current step protocol recorded fast sodium currents within all of these MNs (**Figures 1h** and **2a**). In addition, upon electrical stimulation, patch-clamped Hb9-RFP+ MNs fired action potentials (**Figure 1i**), with strong peak sodium currents of approximately −700 pA (**Figure 1j**). All of these results demonstrate that hESCs require up to 52 days under differentiating conditions for complete functional maturation into a MN.[16–20]

Gene delivery of MN-specifying transcription factors to hESCs results in rapid and efficient generation of MNs

To overcome these barriers related to inefficient and time-intensive MN differentiation from hESCs, we hypothesized that delivery of key MN-specifying transcription factors could rapidly facilitate their differentiation to MNs at a higher efficiency compared to the conventional RA/SHH approach. Based on our temporal gene expression analysis, which identified rate-limiting transcription factors when hESCs were differentiated to MNs upon RA/SHH exposure, we cloned three key MN-specifying genes - *Ngn2*, *Isl-1*, and *Lhx3*. Previous reports have underscored the essential roles of these factors for proper MN development. Specifically, a combinatorial expression of LIM homeodomain transcription factors, Lhx3 and Isl-1, together with the expression of the pro-neural gene, Ngn2, have been shown critical factors to induce MN specification during development.[26–29] Thus, we utilized these factors to efficiently delivery Ngn2, Isl-1, and Lhx3 to our hESC-derived NPCs. We chose adenoviral vectors because of their high infectivity and rapid expression of multiple transgenes within NPCs. Immunohistochemistry revealed that these viruses were capable of infecting hESC-derived NPCs at percentage levels greater than 95% and mediating expression of their respective transcription factor (**Supplementary Figure S4**). Based on this analysis, our adenoviral delivery approach targeted ~85% of cells in culture. We next tested whether these factors could accelerate the differentiation of our hESC-derived NPCs into MNs with greater efficiency compared solely to utilizing RA/SHH-mediated differentiation (**Figure 2a,b**). hESCs were induced into EBs, allowed to adhere to poly-ornithine and laminin-coated dishes, and then differentiated for 10 days into an NPC phenotype. Neural rosette structures were subsequently dissociated and then infected with our cocktail of viruses encoding Ngn2, Isl-1, and Lhx3, and hereafter referred to as N.I.L., at a multiplicity of infectivity of 100. We infected cells at two time points (day 0 and day 4 post NPC differentiation) to increase the efficiency and longevity of expression. In addition, media were supplemented during the differentiation procedure with MN factors including RA, SHH, forskolin, and B27 supplement (**Figure 2b**). Eleven days following infection, we stained cells for phenotypic markers of MNs. At this differentiation stage, cells stained positive for HB9 and CHAT, suggesting that the N.I.L. transcription factors were indeed increasing the rate of MN differentiation within these cells (**Figure 2c**). Nontransduced control hESC-derived NPCs incubated only with RA/SHH for 11 days showed no HB9 or CHAT immunostaining (**Figure 2c**), which is also in agreement with our RT-PCR analysis of temporal gene transcription factor induction during MN differentiation with RA/SHH (**Figure 1c**). To test whether the N.I.L. transcription factors were capable of MN-induced differentiation without any extrinsic neuralizing factors such as RA or SHH, hESC-derived NPCs were infected with N.I.L. and incubated only with B27 supplement to aid in their survival. Without these additional factors, the N.I.L. transcription factors were unable to induce the mature MNs markers, HB9 and CHAT, by this approach, suggesting that the caudalizing effects of RA and ventralizing functions of SHH activate alternate gene expression profiles which are essential for MN differentiation. To verify whether the N.I.L. transcription factors could efficiently direct MN differentiation from an alternative hESC line, we utilized the HuES-3 line, which had been previously engineered with an Hb9::GFP reporter.[12] We utilized the same differentiation protocol as described above, and after 11 days of differentiation, we were able to detect GFP expression within 55% of the cells, demonstrating these cells were efficiently being instructed towards a MN fate (**Figure 2d**). To determine the efficiency of the N.I.L.-directed differentiation approach, we quantified the total number of cells coexpressing HB9 and CHAT. Strikingly, at this early time point, we found that 50 ± 4.5% of our differentiated cells were HB9/CHAT colabeled, indicating that this approach resulted in rapid and efficient generation of MNs (**Figure 2e**). Quantification of MNs generated from the HSF-6 cell line showed 62 ± 2.5% were HB9/CHAT colabeled (**Figure 2e**). Collectively, these results show that MNs can be efficiently and rapidly differentiated from two independent hESC lines by the N.I.L. transcription factor code.

N.I.L. induces predominately cervical and thoracic MN subtypes from hESCs

As hundreds of distinct MN subtypes exist throughout the length of the spinal cord, each responsible for controlling specific muscle groups, we next wanted to identify the MN subtypes that were generated from our N.I.L. induced cells. For this analysis, we applied quantitative PCR to analyze expression of members of the HOX family of transcription factors,[30–33] that dictate cervical, thoracic and lumbar segmental identity phenotypes. Consistent with prior results,[17,18] the default MN phenotype from RA/SHH differentiation is of a cervical phenotype, and our HOX profiling confirmed high expression of cervical markers, including HOXC6, A7, B7, C8, and D8, with low levels of thoracic HOX gene expression and little to no lumbar *HOX* genes

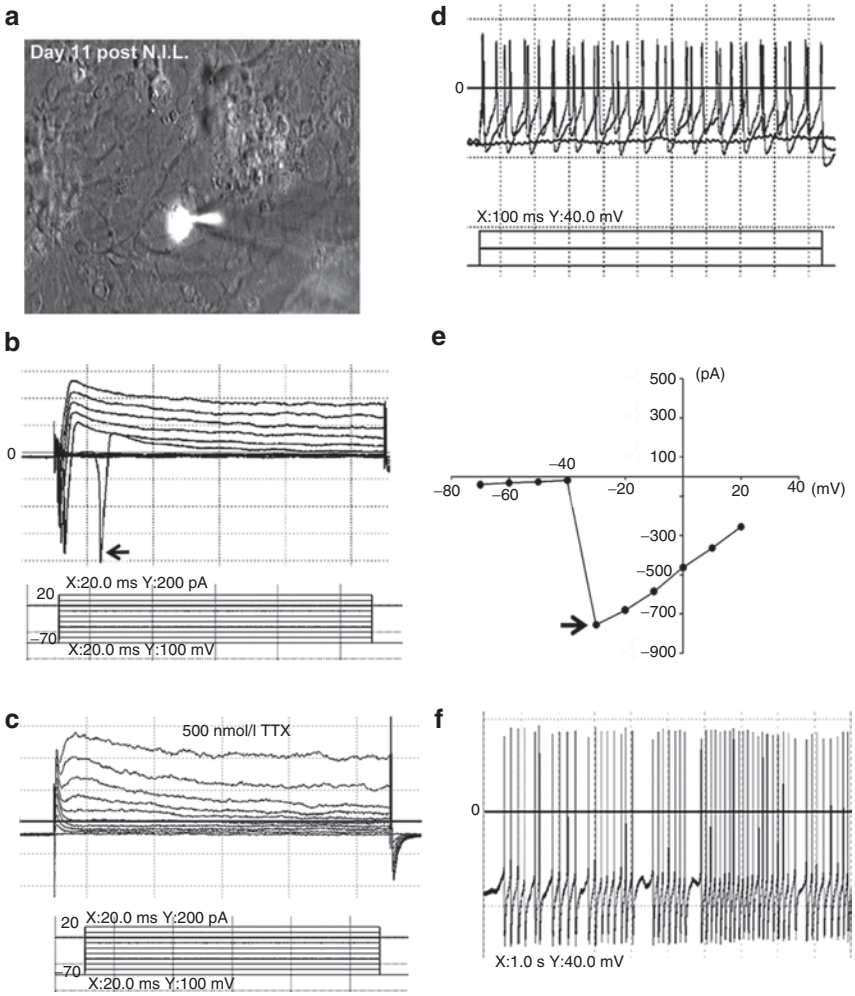

Figure 3 N.I.L.-induced MNs are functionally mature showing characteristic electrophysiological properties. (**a**) N.I.L.-induced MN labeled with *Hb9::RFP* and patch clamped showing sodium current activity (**b**) that could be blocked with tetrodotoxin (TTX) (**c**). N.I.L.-induced MNs displayed action potentials (**d**), peak sodium current activity of approximately –800 pA (**e**), and spontaneous activity (**f**). Arrow in panel "**b**" shows peaks representing sodium currents. Arrow in panel "**e**" shows the peak sodium current activity. MN, motor neurons; N.I.L., Ngn2, Isl-1, and Lhx3.

expressed (Figure 2f). Also as anticipated, the N.I.L. induced cells expressed a very similar profile of HOX gene expression as RA/SHH treated cells, thereby confirming that similar MN subtypes can be generated either from our directed transcription factor based approach or by the conventional RA/SHH treatment protocol (Figure 2f).

N.I.L.-induced MNs form neuromuscular junctions *in vitro*

To further evaluate the functional maturity of the induced MNs, we tested whether these cells could form neuromuscular junctions when cocultured with differentiated C2C12-derived myotubes, which were confirmed to be expressing the mature myotube marker α-actinin (Figure 2g). Within the cocultures, we detected the synaptic marker, synaptic vesicle protein 2, colocalized with TUJ1-positive stained MN axons (Figure 2g). In addition, motor axons colocalizing with acetylcholine receptors on the myotubes were detected with rhodamine-conjugated α-bungarotoxin (Figure 2g), further indicating that the MNs were capable of forming neuromuscular junctions.

N.I.L.-induced MNs acquire electrophysiological properties in a rapid time frame

We next evaluated the functional maturity of the MNs by measuring their electrophysiological properties 11 days post-transduction with the N.I.L. cocktail. To visualize MNs, we infected cells with the previously described lentivirus containing an *Hb9::RFP* reporter and were then transferred to a layer of astrocytes for an additional 4 days before electrophysiological measurements were performed. A total of 10 RFP-positive MNs, differentiated from the HSF-6 cell line, were patch-clamped (Figure 3a), and electrophysiological measurements demonstrated strong sodium currents (Figure 3b), indicative of MN electrophysiological properties in all recorded MNs. Sodium channel currents could also be blocked by administration of 500 nmol/l tetrodotoxin (Figure 3c), further demonstrating the specificity of sodium current channel measurements. In addition, the MNs demonstrated action potentials upon electrical stimulation, indicating their functional maturity (Figure 3d). Sodium current were measured at approximately –800 pA (Figure 3e), with the additional capacity for strong spontaneous activity (Figure 3f). Collectively, these results demonstrate

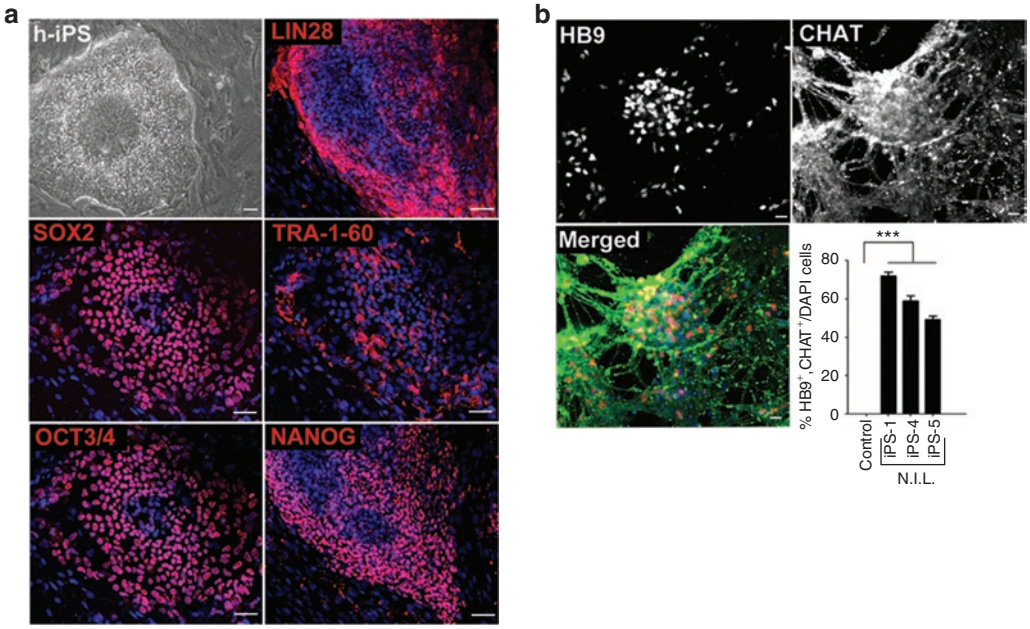

Figure 4 N.I.L.-induces rapid and efficient generation of MNs from hiPSCs. (**a**) Phase contrast picture of a hiPSC clone showing distinct hESC morphology. hiPSCs express markers associated with pluripotency such as LIN28, OCT3/4, SOX2, TRA-1-60, and NANOG. (**b**) N.I.L.-induced MNs express HB9 and CHAT, and are colocalized in the same cells merged with the nuclear dye, DAPI. Quantification of induced MNs colabeled with HB9/CHAT from hiPS cells. In panel "**a**" bars = 100 µm. In panel "**b**" bars = 50 µm. hESC, human embryonic stem cell; hiPSCs, human induced pluripotent stem cells; MN, motor neurons; N.I.L., Ngn2, Isl-1, and Lhx3.

that the N.I.L. instruction rapidly produced MNs with the electrophysiological competence of mature MNs.

N.I.L. induces MNs rapidly and efficiently from hiPSCs

Given the success of using N.I.L. on hESCs for rapidly and efficiently generating electrophysiologically-competent MNs, we next planned to determine whether the same approach could be utilized to generate MNs from human induced pluripotent stem cells (hiPSCs). Numerous reports have demonstrated that hiPSCs can be derived from multiple cell types utilizing various transcription factor cocktail combinations.[34–41] We derived a line of hiPSCs from human fibroblasts using retroviral vectors expressing the four Yamanaka factors (OCT3/4, KLF-4, SOX2, and c-MYC)[42] (**Figure 4a**). The hiPSCs were stained with LIN28, OCT3/4, SOX2, TRA-1-60, and NANOG to confirm that they expressed pluripotent characteristics (**Figure 4a**). These cells were then exposed to the same protocol that we used on hESCs and described in **Figure 2b**. Similar to the previously described protocol for the N.I.L. induction of MNs, cells were transduced with adenoviruses expressing N.I.L. and evaluated 11 days later for MN markers. The cells exhibited robust MN differentiation, with 72 ± 3.4% of the cells colabeled with HB9 and CHAT (**Figure 4b**). Previous studies have shown that iPS lines could vary in their ability to differentiate into mature cell types.[43] Therefore, we tested two additional iPS lines for their ability to become efficiently differentiated into MNs utilizing our N.I.L. induction strategy.[44] Similar to our previous results, we were able to achieve similar MN differentiation efficiencies within iPS lines 4 and 5 showing 59 ± 4.2% and 49 ± 3.3% colabeling with HB9 and CHAT, respectively (**Supplementary Figure S5**, **Figure 4b**). Consistent with our previous results on hESC differentiation into MNs with RA/SHH, nontransduced control cells did not stain positive for HB9 or CHAT at this early time point in differentiation. These results further exemplify the utility of the N.I.L directed programming approach on multiple hiPS cell lines showing highly efficient and rapid generation of MNs (**Figure 4b**).

DISCUSSION

Pluripotent cells have proven to be an invaluable stem cell source for deriving MNs. However, generating MNs is time intensive and current approaches yield 10–40% MN differentiation along with a heterogeneous population of neuronal and non-neuronal cells.[16–21] In part, this heterogeneity is caused by the way in which RA and SHH impart neuronal diversity within the embryonic spinal cord.[45] To more accurately and efficiently guide hESCs into MNs, we utilized critical MN-specifying transcription factors that act downstream of RA/SHH signaling.[29] Our results demonstrate that MN-specifying transcription factors are capable of producing functional MNs in a rapid and efficient manner. A future direction for this technology would be to program alternate neuronal types that exist throughout the CNS. Indeed, recent work has shown that delivery of a critical transcription factor, Lmx1a, to hES cells can direct their differentiation into mesencephalic dopaminergic neurons.[46] In addition, it may be possible to use transcription factor codes to generate alternate MN subtype fates such as those that innervate limb muscles.

Although we have not observed any untoward effects of sustained expression of these factors within MNs, it will be of interest to determine whether the MN genetic program is retained after silencing viral-mediated transcription factor expression postdifferentiation. Furthermore, we have observed that N.I.L.-directed MNs could survive up to 6 weeks in culture demonstrating their high applicability as a drug screening tool.

MNs have been increasingly utilized to model neurodegenerative diseases *in vitro* such as SMA and ALS.[5,8–13] For example, Ebert *et al.* demonstrated that MNs differentiated from iPS cells, which were derived from an SMA patient, showed that SMA MNs exhibited shortened neurite extensions and decreased survival in culture compared to healthy MNs.[5] Additional reports modeling ALS *in vitro* have exemplified the susceptibility of MNs to ALS-derived astrocytes.[8–13] Although ALS patient-derived MNs have been generated through iPS cell technology,[47,48] no report has documented any defect in these MNs. To overcome the technical challenges of generating MNs from large numbers of iPS lines from patients with MN disease, a more rapid and efficient method of MN differentiation would be highly invaluable to stem cell biologists over currently available techniques. Our induced MN differentiation method from either hES or iPS cells bypasses these technical constraints of MN differentiation by generating a large supply of these cells within a rapid and accelerated time frame. We envision this technology would be highly applicable for drug screening platforms for MN disease such as SMA or ALS. Pluripotent stem cell lines could be engineered with an Hb9::GFP or Hb9::luciferase reporter system for monitoring and quantification purposes during the drug screening process. In addition, toxicology studies could also be performed on highly enriched MNs to test for candidate drug targets.

In sum, this transcriptional coding strategy allows for the generation of functional MNs with characteristic electrophysiological properties at high efficiency within ~11 days from hESCs or hiPSCs, a strategy that should prove valuable to those studying basic MN biology *in vitro*, developing screening assays for MN disease, or advancing applications in regenerative medicine.

MATERIALS AND METHODS

Cell culture. The HSF-6 hESC line (P65) was obtained from the National Stem Cell Bank (NSCB) and was cultured and passaged on irradiated primary mouse embryonic fibroblasts (Millipore, Billerica, MA) as previously described.[49] hiPSCs were cultured similarly to hESCs. Human iPS lines, iPS-4 and iPS-5, were obtained from Children's Hospital Boston Stem Cell Program, George Q. Daley's laboratory. The HuES-3 Hb9::GFP cell line was a kind gift from Kevin Eggan (Harvard University, Cambridge, MA).

Adenoviral and lentiviral constructs. The AdEasy Adenoviral Vector System (Stratagene, La Jolla, CA) was utilized to construct adenoviruses for the mouse *Lhx3*, *Isl1*, and *Ngn2* genes. All cDNAs corresponding to the coding regions of these genes were subcloned into the *Bam*HI and *Xho* I sites of the pShuttle-CMV adenoviral vector, and all subsequent steps were performed according to the manufacturer's instructions using human 293 cells for viral propagation. Viral titers were between 10^{11} and 10^{12} viral particles/ml, as determined by the $TCID_{50}$ assay.

A lentiviral reporter construct driving RFP under the control of the *Hb9* promoter (kind gift of Sam Pfaff, Carol Marchetto, and Fred Gage) was utilized to identify MNs. Lentivirus, pseudotyped with vesicular stomatis virus glycoprotein, was produced by quadruple transfection in HEK-293 cells, as previously described.[50]

hiPSC generation. pMXs retroviral vectors (Addgene, Cambridge, MA) encoding OCT3/4, SOX2, KLF-4, and c-MYC were transfected using the $CaCl_2$ method separately with CMV-GP and VSVG plasmids into human embryonic kidney carcinoma 293 cells (HEK-293) to produce retroviruses. Forty-eight hours postinfection, supernatant was collected, mixed, and filtered through a 0.22-micron filter and supplemented with polybrene at 5 μg/ml. 60,000 normal fibroblasts (Coriell, Camden, NJ) were infected with retroviruses on a 10 cm^2 tissue culture plate. Media was changed to Dulbecco's modified Eagle's medium supplemented with 10% fetal bovine serum and cells were allowed to grow for 1 week until media was changed to hESC media supplemented with the rho kinase inhibitor, Y-27632 (Calbiochem, Gibbston, NJ).

Karyotyping. Karyotyping of the HSF6 hESC line was performed at the Molecular Cytogenetics shared resource at the Ohio State University Comprehensive Cancer Center.

qRT-PCR. RNA was harvested from proliferating hESCs, RA/SHH-induced, and N.I.L.-induced MNs. Total RNA was reverse transcribed with RT² First Strand Kit (SABiosciences, Frederick, MD) according to the manufacturer's instructions. Real-time quantitative PCR reactions were performed using RT² Real-Time SYBR Green/Rox PCR Master Mix (SABiosciences) and run on an RT² Profiler PCR Array for Human HOX genes (SABiosciences). Primers used in this study are shown in **Supplementary Table S1**.

MN differentiation. To induce MN differentiation, hESC or iPSC colonies were first removed from a mouse feeder layer with 1 mg/ml collagenase IV. Colonies were then resuspended in Dulbecco's modified Eagle's medium/F12 supplemented with 1% N2 and 10% knockout serum (Invitrogen, Carlsbad, CA), and plated within a Petri dish to induce embryoid body formation for the first 2 days. After 2 days of incubation, serum-free media was utilized as described above without 10% knockout serum for an additional 2 days. After 4 days of differentiation, EBs were then allowed to attach as distinct noncontacting colonies to polyornithine/laminin coated dishes for an additional 6 days to induce the formation of neural rosettes. Neural rosettes were then manually removed by a small pipettor, dissociated with accutase (Invitrogen), plated on poly-ornithine/laminin coated dishes, and then treated either with RA (2 μmol/l) and SHH (500 ng/ml), for conventional MN differentiation.

N.I.L.-induced MN differentiation. NPCs were differentiated from hESCs or iPSCs by the same protocol as described above. After 10 days of differentiation into neural rosettes containing NPCs, neural rosettes were manually removed with a pipettor, dissociated, and plated on poly-ornithine/laminin coated dishes as described above. After 24 hours, NPCs were infected with N.I.L., which is considered day 1 on the differentiation timeline (**Figure 2a–b**) (multiplicity of infection = 100), and supplemented with RA (2 μmol/l), forskolin (5 μmol/l), SHH (500 ng/ml), and B27 (0.2%). On day 4, NPCs were infected an additional time at a similar multiplicity of infection and supplemented with the same factors as described above.

Myotube coculture experiments. C2C12 cells were differentiated in 10% horse serum to induce myotube formation. MNs were then plated to the myotube monolayer and showed the neuromuscular synapses within 1 week of coculture.

Immunocytochemistry and alkaline phosphatase activity staining. Cells were stained with the antibodies shown in **Supplementary Table S1**. All images were captured using a Zeiss LSM510-META confocal laser-scanning microscope (Zeiss, Thornwood, NY). Staining for alkaline phosphatase activity was performed using the alkaline phosphatase activity kit (Millipore).

Electrophysiology recording. Whole-cell patch recordings were performed from hESC-derived MNs that express *Hb9::RFP*. The recording micropipettes were pulled to have tip resistance of 2–4 MΩ when filled with an internal solution (115 mmol/l K-gluconate, 4 mmol/l NaCl, 1.5 mmol/l $MgCl_2$, 20 mmol/l HEPES, and 0.5 mmol/l EGTA, pH 7.3) and placed in a bath solution (115 mmol/l NaCl, 2 mmol/l KCl, 10 mmol/l HEPES, 3 mmol/l $CaCl_2$, 10 mmol/l glucose, and 1.5 mmol/l $MgCl_2$, pH 7.3). Recordings were made using a EPC10 amplifier (HEKA Instruments, Southboro, MA). Signals were filtered at 3 kHz and sampled at 20 kHz. The whole-cell capacitance

was fully compensated, whereas the series resistance was uncompensated but monitored during the experiment by the amplitude of the capacitive current in response to a 5-mV pulse. For current-clamp recordings, cells were either held at the level without current injection to observe resting membrane potential and spontaneous firing or held at −60 ~ −70 mV level through current injection prior to the current step protocol. For voltage-clamp recordings, cells were clamped at −70 mV before the voltage step protocol was performed. All recordings were performed at room temperature.

SUPPLEMENTARY MATERIAL

Figure S1. HSF-6 hESCs show a normal 46XX karyotype.
Figure S2. The HSF-6 hESC line shows markers of pluripotency.
Figure S3. HSF-6 hESCs transit through progenitor cell intermediates towards a MN fate.
Figure S4. Adenoviral transcription factors Ngn2, Isl-1, and Lhx3 can infect hESC-derived NPCs.
Figure S5. N.I.L.-induced MNs express HB9 and CHAT, and are co-localized in the same cells merged with the nuclear dye, DAPI in iPS lines 4 and 5.
Table S1. All antibodies and sequences of primers utilized in this study.

ACKNOWLEDGMENTS

We are thankful to Kevin Eggan for providing the HuES-3 Hb9::GFP cell line. This work was funded by NIH R01 NS6449l2-1A1, RC2 NS69476-01, Helping Link Foundation to B.K.K., The Ohio State University Electrophysiology Core supported by NINDS core grant P30 NS045758., and Project A.L.S. to F.H.G. and B.K.K. and F.H.G. is supported in part by California Institute for Regenerative Medicine (CIRM). K.M. is supported by a fellowship from the Swiss National Science Foundation (SNSF), and C.J.M. is supported by a fellowship from the Craig H. Neilsen Foundation.

REFERENCES

1. Foust, KD, Wang, X, McGovern, VL, Braun, L, Bevan, AK, Haidet, AM *et al.* (2010). Rescue of the spinal muscular atrophy phenotype in a mouse model by early postnatal delivery of SMN. *Nat Biotechnol* **28**: 271–274.
2. Dominguez, E, Marais, T, Chatauret, N, Benkhelifa-Ziyyat, S, Duque, S, Ravassard, P *et al.* (2011). Intravenous scAAV9 delivery of a codon-optimized SMN1 sequence rescues SMA mice. *Hum Mol Genet* **20**: 681–693.
3. Passini, MA, Bu, J, Roskelley, EM, Richards, AM, Sardi, SP, O'Riordan, CR *et al.* (2010). CNS-targeted gene therapy improves survival and motor function in a mouse model of spinal muscular atrophy. *J Clin Invest* **120**: 1253–1264.
4. Valori, CF, Ning, K, Wyles, M, Mead, RJ, Grierson, AJ, Shaw, PJ *et al.* (2010). Systemic delivery of scAAV9 expressing SMN prolongs survival in a model of spinal muscular atrophy. *Sci Transl Med* **2**: 35ra42.
5. Ebert, AD, Yu, J, Rose, FF Jr, Mattis, VB, Lorson, CL, Thomson, JA *et al.* (2009). Induced pluripotent stem cells from a spinal muscular atrophy patient. *Nature* **457**: 277–280.
6. Rossi, SL, Nistor, G, Wyatt, T, Yin, HZ, Poole, AJ, Weiss, JH *et al.* (2010). Histological and functional benefit following transplantation of motor neuron progenitors to the injured rat spinal cord. *PLoS ONE* **5**: e11852.
7. Corti, S, Nizzardo, M, Nardini, M, Donadoni, C, Salani, S, Ronchi, D *et al.* (2008). Neural stem cell transplantation can ameliorate the phenotype of a mouse model of spinal muscular atrophy. *J Clin Invest* **118**: 3316–3330.
8. Nagai, M, Re, DB, Nagata, T, Chalazonitis, A, Jessell, TM, Wichterle, H *et al.* (2007). Astrocytes expressing ALS-linked mutated SOD1 release factors selectively toxic to motor neurons. *Nat Neurosci* **10**: 615–622.
9. Di Giorgio, FP, Carrasco, MA, Siao, MC, Maniatis, T and Eggan, K (2007). Non-cell autonomous effect of glia on motor neurons in an embryonic stem cell-based ALS model. *Nat Neurosci* **10**: 608–614.
10. Dodge, JC, Haidet, AM, Yang, W, Passini, MA, Hester, M, Clarke, J *et al.* (2008). Delivery of AAV-IGF-1 to the CNS extends survival in ALS mice through modification of aberrant glial cell activity. *Mol Ther* **16**: 1056–1064.
11. Dodge, JC, Treleaven, CM, Fidler, JA, Hester, M, Haidet, A, Handy, C *et al.* (2010). AAV4-mediated expression of IGF-1 and VEGF within cellular components of the ventricular system improves survival outcome in familial ALS mice. *Mol Ther* **18**: 2075–2084.
12. Di Giorgio, FP, Boulting, GL, Bobrowicz, S and Eggan, KC (2008). Human embryonic stem cell-derived motor neurons are sensitive to the toxic effect of glial cells carrying an ALS-causing mutation. *Cell Stem Cell* **3**: 637–648.
13. Marchetto, MC, Muotri, AR, Mu, Y, Smith, AM, Cezar, GG and Gage, FH (2008). Non-cell-autonomous effect of human SOD1 G37R astrocytes on motor neurons derived from human embryonic stem cells. *Cell Stem Cell* **3**: 649–657.
14. Wichterle, H, Lieberam, I, Porter, JA and Jessell, TM (2002). Directed differentiation of embryonic stem cells into motor neurons. *Cell* **110**: 385–397.
15. Briscoe, J and Ericson, J (2001). Specification of neuronal fates in the ventral neural tube. *Curr Opin Neurobiol* **11**: 43–49.
16. Singh Roy, N, Nakano, T, Xuing, L, Kang, J, Nedergaard, M and Goldman, SA (2005). Enhancer-specified GFP-based FACS purification of human spinal motor neurons from embryonic stem cells. *Exp Neurol* **196**: 224–234.
17. Lee, H, Shamy, GA, Elkabetz, Y, Schofield, CM, Harrsion, NL, Panagiotakos, G *et al.* (2007). Directed differentiation and transplantation of human embryonic stem cell-derived motoneurons. *Stem Cells* **25**: 1931–1939.
18. Li, XJ, Du, ZW, Zarnowska, ED, Pankratz, M, Hansen, LO, Pearce, RA *et al.* (2005). Specification of motoneurons from human embryonic stem cells. *Nat Biotechnol* **23**: 215–221.
19. Shin, S, Dalton, S and Stice, SL (2005). Human motor neuron differentiation from human embryonic stem cells. *Stem Cells Dev* **14**: 266–269.
20. Lim, UM, Sidhu, KS and Tuch, BE (2006). Derivation of Motor Neurons from three Clonal Human Embryonic Stem Cell Lines. *Curr Neurovasc Res* **3**: 281–288.
21. Hu, BY and Zhang, SC (2009). Differentiation of spinal motor neurons from pluripotent human stem cells. *Nat Protoc* **4**: 1295–1304.
22. Dhara, SK and Stice, SL (2008). Neural differentiation of human embryonic stem cells. *J Cell Biochem* **105**: 633–640.
23. Wu, H, Xu, J, Pang, ZP, Ge, W, Kim, KJ, Blanchi, B *et al.* (2007). Integrative genomic and functional analyses reveal neuronal subtype differentiation bias in human embryonic stem cell lines. *Proc Natl Acad Sci USA* **104**: 13821–13826.
24. Miles, GB, Yohn, DC, Wichterle, H, Jessell, TM, Rafuse, VF and Brownstone, RM (2004). Functional properties of motoneurons derived from mouse embryonic stem cells. *J Neurosci* **24**: 7848–7858.
25. Johnson, MA, Weick, JP, Pearce, RA and Zhang, SC (2007). Functional neural development from human embryonic stem cells: accelerated synaptic activity via astrocyte coculture. *J Neurosci* **27**: 3069–3077.
26. Lee, SK and Pfaff, SL (2001). Transcriptional networks regulating neuronal identity in the developing spinal cord. *Nat Neurosci* **4 Suppl**: 1183–1191.
27. Pfaff, SL, Mendelsohn, M, Stewart, CL, Edlund, T and Jessell, TM (1996). Requirement for LIM homeobox gene Isl1 in motor neuron generation reveals a motor neuron-dependent step in interneuron differentiation. *Cell* **84**: 309–320.
28. Thaler, JP, Lee, SK, Jurata, LW, Gill, GN and Pfaff, SL (2002). LIM factor Lhx3 contributes to the specification of motor neuron and interneuron identity through cell-type-specific protein-protein interactions. *Cell* **110**: 237–249.
29. Shirasaki, R and Pfaff, SL (2002). Transcriptional codes and the control of neuronal identity. *Annu Rev Neurosci* **25**: 251–281.
30. Dasen, JS, De Camilli, A, Wang, B, Tucker, PW and Jessell, TM (2008). Hox repertoires for motor neuron diversity and connectivity gated by a single accessory factor, FoxP1. *Cell* **134**: 304–316.
31. Dasen, JS, Tice, BC, Brenner-Morton, S and Jessell, TM (2005). A Hox regulatory network establishes motor neuron pool identity and target-muscle connectivity. *Cell* **123**: 477–491.
32. Dasen, JS, Liu, JP and Jessell, TM (2003). Motor neuron columnar fate imposed by sequential phases of Hox-c activity. *Nature* **425**: 926–933.
33. Rousso, DL, Gaber, ZB, Wellik, D, Morrisey, EE and Novitch, BG (2008). Coordinated actions of the forkhead protein Foxp1 and Hox proteins in the columnar organization of spinal motor neurons. *Neuron* **59**: 226–240.
34. Aoki, T, Ohnishi, H, Oda, Y, Tadokoro, M, Sasao, M, Kato, H *et al.* (2010). Generation of induced pluripotent stem cells from human adipose-derived stem cells without c-MYC. *Tissue Eng Part A* **16**: 2197–2206.
35. Hester, ME, Song, S, Miranda, CJ, Eagle, A, Schwartz, PH and Kaspar, BK (2009). Two factor reprogramming of human neural stem cells into pluripotency. *PLoS ONE* **4**: e7044.
36. Yu, J, Vodyanik, MA, Smuga-Otto, K, Antosiewicz-Bourget, J, Frane, JL, Tian, S *et al.* (2007). Induced pluripotent stem cell lines derived from human somatic cells. *Science* **318**: 1917–1920.
37. Kim, JB, Greber, B, Araúzo-Bravo, MJ, Meyer, J, Park, KI, Zaehres, H *et al.* (2009). Direct reprogramming of human neural stem cells by OCT4. *Nature* **461**: 649–643.
38. Nakagawa, M, Koyanagi, M, Tanabe, K, Takahashi, K, Ichisaka, T, Aoi, T *et al.* (2008). Generation of induced pluripotent stem cells without Myc from mouse and human fibroblasts. *Nat Biotechnol* **26**: 101–106.
39. Haase, A, Olmer, R, Schwanke, K, Wunderlich, S, Merkert, S, Hess, C *et al.* (2009). Generation of induced pluripotent stem cells from human cord blood. *Cell Stem Cell* **5**: 434–441.
40. Kaji, K, Norrby, K, Paca, A, Mileikovsky, M, Mohseni, P and Woltjen, K (2009). Virus-free induction of pluripotency and subsequent excision of reprogramming factors. *Nature* **458**: 771–775.
41. Kim, JB, Zaehres, H, Araúzo-Bravo, MJ and Schöler, HR (2009). Generation of induced pluripotent stem cells from neural stem cells. *Nat Protoc* **4**: 1464–1470.
42. Takahashi, K, Tanabe, K, Ohnuki, M, Narita, M, Ichisaka, T, Tomoda, K *et al.* (2007). Induction of pluripotent stem cells from adult human fibroblasts by defined factors. *Cell* **131**: 861–872.
43. Bock, C, Kiskinis, E, Verstappen, G, Gu, H, Boulting, G, Smith, ZD *et al.* (2011). Reference Maps of human ES and iPS cell variation enable high-throughput characterization of pluripotent cell lines. *Cell* **144**: 439–452.
44. Park, IH, Arora, N, Huo, H, Maherali, N, Ahfeldt, T, Shimamura, A *et al.* (2008). Disease-specific induced pluripotent stem cells. *Cell* **134**: 877–886.
45. Jessell, TM (2000). Neuronal specification in the spinal cord: inductive signals and transcriptional codes. *Nat Rev Genet* **1**: 20–29.
46. Friling, S, Andersson, E, Thompson, LH, Jönsson, ME, Hebsgaard, JB, Nanou, E *et al.* (2009). Efficient production of mesencephalic dopamine neurons by Lmx1a expression in embryonic stem cells. *Proc Natl Acad Sci USA* **106**: 7613–7618.
47. Dimos, JT, Rodolfa, KT, Niakan, KK, Weisenthal, LM, Mitsumoto, H, Chung, W *et al.* (2008). Induced pluripotent stem cells generated from patients with ALS can be differentiated into motor neurons. *Science* **321**: 1218–1221.
48. Boulting, GL, Kiskinis, E, Croft, GF, Amoroso, MW, Oakley, DH, Wainger, BJ *et al.* (2011). A functionally characterized test set of human induced pluripotent stem cells. *Nat Biotechnol* **29**: 279–286.
49. Thomson, JA, Itskovitz-Eldor, J, Shapiro, SS, Waknitz, MA, Swiergiel, JJ, Marshall, VS *et al.* (1998). Embryonic stem cell lines derived from human blastocysts. *Science* **282**: 1145–1147.
50. Kafri, T, Blömer, U, Peterson, DA, Gage, FH and Verma, IM (1997). Sustained expression of genes delivered directly into liver and muscle by lentiviral vectors. *Nat Genet* **17**: 314–317.